JTTEE5 14:391-396
DOI: 10.1361/105996305X59404
1059-9630/$19.00 © ASM International

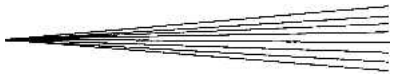

Optimal Design of a Novel Cold Spray Gun Nozzle at a Limited Space

Wen-Ya Li and Chang-Jiu Li

(Submitted July 1, 2004; in revised form November 29, 2004)

Numerical analysis for the accelerating behavior of spray particles in cold spraying is conducted using a computational fluid dynamics program, FLUENT. The optimal design of the spray gun nozzle is achieved based on simulation results to solve the problem of coating for the limited inner wall of a small cylinder or pipe. It is found that the nozzle expansion ratio, particle size, accelerating gas type, operating pressure, and temperature are main factors influencing the accelerating behavior of spray particles in a limited space. The experimental results using the designed short nozzle with a whole gun length of <70 mm confirmed the feasibility of optimal design for a spray gun nozzle used in a limited space.

Keywords accelerating behavior, cold spraying, nozzle, numerical analysis, optimal design, particle

1. Introduction

Cold spraying, also termed *cold gas-dynamic spray*, is a new emerging coating technology. In this process, spray particles (1-50 μm in size) are accelerated by a supersonic jet of compressed gas to a high velocity (300-1200 m/s) and impact on a substrate at a temperature that is always lower than the melting point of the material, resulting in a coating formation constructed from completely solid particles (Ref 1). As shown in Fig. 1 (Ref 2), the supersonic jet is generated through a converging-diverging de Laval nozzle. The accelerating gas is usually preheated to a temperature <700 °C depending on the spray materials before it is introduced into the spray gun from the gas inlet (Ref 1). Spray particles are fed into the supersonic jet axially from the back of the spray gun. The operating temperature and the pressure of the accelerating gas are monitored by the thermocouple and pressure gauge mounted on the spray gun. As a result, the phenomena inherent to thermal spraying at high temperatures, such as oxidation and phase transformation, can be avoided in cold spraying.

The most important parameter for a spray particle in cold spraying is its velocity prior to impact. It is generally accepted that there exists a critical velocity for successful particle deposition with a given spray material (Ref 1). Only the particles moving at a velocity higher than the critical one can be deposited to produce a coating. Therefore, it is essential to understand the accelerating behavior of a spray particle.

Although the measurement of particle velocity is feasible (Ref 3), it is not an efficient and cost-effective approach to undertaking a systematic investigation. The progress in computational fluid dynamics has made it possible to simulate gas-solid two-phase flow precisely. The simulation result attained by assuming a one-dimensional isentropic flow showed good agreement with the experimental results (Ref 3). Based on the simple one-dimensional isentropic model, it was indicated that particle velocity in cold spraying could be influenced by the nozzle expansion ratio (i.e., the ratio of the area of the exit to the throat) (Ref 4), the entrance convergent section length (Ref 5), the driving gas conditions (Ref 4-7), and the particle density and size (Ref 4-6, 8). Jodoin (Ref 9) reported the effect of shock waves

Wen-Ya Li, LERMPS-UTBM, Sité de Sévenans, 90400, Belfort-Cedex France, and **Chang-Jiu Li,** State Key Laboratory for Mechanical Behavior of Materials, Welding Research Institute, School of Materials Science and Engineering, Xi'an Jiaotong University, Xi'an, Shaanxi, 710049, Peoples Republic of China. Contact e-mail: wenyali_cn@hotmail.com.

Table of Symbols

D_i	nozzle inlet diameter, mm
D_t	nozzle throat diameter, mm
D_e	nozzle exit diameter, mm
L_u	nozzle upstream length, mm
L_d	nozzle downstream length, mm
V_p	particle velocity, m/s
V_g	gas velocity, m/s
ρ_p	particle density, kg/m^3
ρ_g	gas density, kg/m^3
d_p	particle diameter, m
C_d	drag coefficient
a_1	constant defining C_d
a_2	constant defining C_d
a_3	constant defining C_d
Re	Reynolds number
μ_g	dynamic viscosity of gas, kg/m/s
T_p	particle temperature, K
T_g	gas temperature, K
$C_{p\text{-}p}$	heat capacity of particle, J/kg/K
$C_{p\text{-}g}$	heat capacity of gas, J/kg/K
h	heat transfer coefficient, W/m^2/K
λ_g	thermal conductivity of gas, W/m/K
Nu	Nusselt number
Pr	Prandtl number
Bi	Biot number
M	Mach number
γ	specific heat ratio of gas
R	specific gas constant, J/kg/K

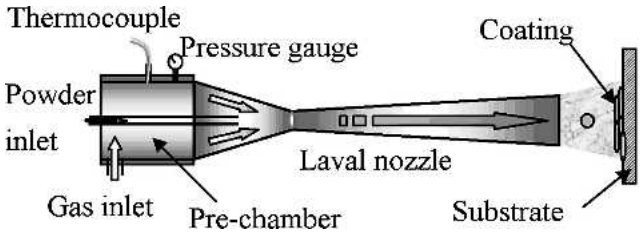

Fig. 1 Schematic diagram of cold spray gun

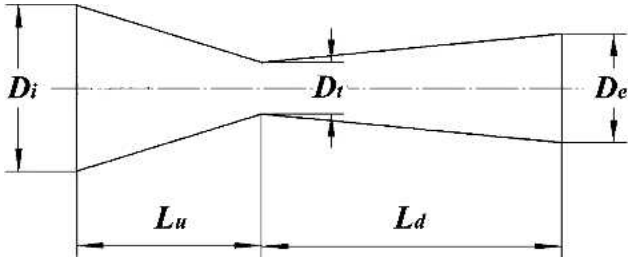

Fig. 2 Schematic diagram of the nozzle geometry

outside the nozzle exit on particle acceleration and pointed out that there was a limitation in nozzle design Mach number. On the other hand, FLUENT was proven to be reliable for modeling the gas flow in a Laval nozzle through experimental validation (Ref 9). The previous numerical study using FLUENT showed that the nozzle divergent section length significantly influences the particle velocity as well as the gas conditions (Ref 10). The nozzle expansion ratio presented an optimal value of ~4 with regard to particle velocity at a standoff distance of 20 mm as the divergent section length is 100 mm, whereas other dimensions defining the nozzle geometry have little effect on particle acceleration. On the other hand, the standoff distance takes a significant role in determining particle velocity as the nozzle divergent length is relatively short, especially <50 mm (Ref 10). However, in the current study, the divergent section length is restricted by the limited space. Although the applications of thermal spray in coating internal diameters, such as plasma spray (Ref 11) and high-velocity oxyfuel spray (Ref 12), have been successfully developed, there are few reports concerning the coatings for internal diameters.

Therefore, the aim of this present study was to design the short cold spray gun nozzle by finite-element analysis and to seek some effective methods for improving particle velocity for applications in limited internal diameters.

2. Modeling

2.1 Parameters Involved in Simulation

In this study, three sets of parameters are mainly involved in the simulation: the geometry of spray gun nozzle; driving gas conditions; and powder parameters.

The geometry of the converging-diverging nozzle used in this simulation is given schematically in Fig. 2. Both the converging and diverging sections of the spray gun nozzle have a conical shape in a circular section along the axis. Five parameters are used to define the geometry of the spray gun nozzle. These parameters are nozzle inlet diameter, throat diameter, exit diameter, upstream length (converging section), and downstream length (diverging section). Based on the previous experimental study (Ref 2), the geometric parameters of the nozzle selected for simulation are shown in Table 1. In this study, only exit diameter is changed to adjust the nozzle expansion ratio.

Nitrogen (N_2) and helium (He) are used as driving gases. The gas pressure was changed from 1 to 3 MPa, and the gas temperature ranged from 27 to 600 °C.

In cold spraying, the type of material used in the powder, and its morphology, size, and size distribution will influence the acceleration of spray particles (Ref 10). In this study, spherical copper particles are used as feedstock with a particle diameter ranging from 5 to 50 μm.

Table 1 The nozzle dimensions used in simulation

Nozzle parameters	Values, mm
D_i	8
D_t	2
D_e	2, 3, 4, 5, 6, 7, 8
L_u	10
L_d	40

2.2 Numerical Simulation Method

Numerical simulation is carried out by using the commercial software FLUENT (Fluent Inc., Lebanon, NH) to determine the flow field of the driving gas inside and outside the nozzle, and subsequently the accelerating and heating of particles in the cold spray. Owing to the axisymmetrical characteristic of the flow in this study, a two-dimensional model is used. A schematic diagram of the computational domain and boundaries is shown in Fig. 3. For the precise determination of particle velocity prior to impact, the domain is extended to a cylinder of 60 mm in radius and 200 mm in length outside the nozzle exit. The computational domain is meshed using a regular and structured grid of quadrilateral elements. The standoff distance from nozzle exit to substrate surface is 30 mm.

The governing equations for gas flow include the physical laws of conservation of mass, momentum, and energy. The standard K-ε turbulence model is used. The gas is taken as an ideal and compressible one. A coupled implicit method is used to solve the flow field, and results for the flow field in a steady state are obtained. A second-order discretization scheme is used. The accelerating and heating of particles are computed using the discrete phase modeling (DPM) of FLUENT (Ref 13). The interaction of the particle with the gas flow is not considered in this study.

Models describing the dynamic and thermal behavior of in-flight particles during the two-phase flow have been well-documented in the FLUENT manual (Ref 13). The acceleration of a spherical particle by a fluid flow can be expressed by the following equation:

$$\frac{dV_p}{dt} = \frac{3C_d\rho_g}{4d_p\rho_p}(V_g - V_p)|V_g - V_p| \quad \text{(Eq 1)}$$

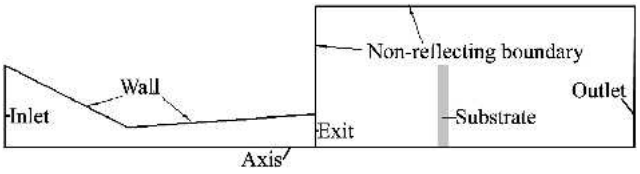

Fig. 3 Schematic diagram of the computational domain and boundaries

For a smooth spherical particle, C_d is given by:

$$C_d = a_1 + \frac{a_2}{Re} + \frac{a_3}{Re} \quad \text{(Eq 2)}$$

The Reynolds number (Re) is defined by:

$$Re = \frac{\rho_g d_p |V_g - V_p|}{\mu_g} \quad \text{(Eq 3)}$$

This equation can be practically applied to a *Re* of <50,000.

Regarding the thermal behavior of the metallic particles, it is assumed that heat conduction within a particle is neglected, and the particle is therefore treated as isothermal. The heating rate is described by:

$$\frac{dT_p}{dt} = \frac{6h}{C_{p-p}\rho_p d_p}(T_g - T_p) \quad \text{(Eq 4)}$$

The heat transfer coefficient is related to the thermal conductivity of gas fluid by Nusselt number as follows:

$$h = \frac{\lambda_g Nu}{d_p} \quad \text{(Eq 5)}$$

Nusselt number is given by:

$$Nu = 2 + 0.6 Pr^{1/3} Re^{1/2} \quad \text{(Eq 6)}$$

Prandtl number is described as:

$$Pr = \frac{\mu_g C_{p-g}}{\lambda_g} \quad \text{(Eq 7)}$$

In the simulation, the particles are introduced axially from the nozzle inlet with an initial velocity of 50 m/s and a temperature of 27 °C. For gas flow, the reference atmosphere is at a pressure of 0.1 MPa and the temperature of 27 °C.

3. Simulation Results

3.1 Effect of Nozzle Expansion Ratio on Particle Acceleration

Figure 4 shows the effect of nozzle exit diameter on the particle velocity at the standoff distance with different particle diameters using N_2 as the accelerating gas at a pressure of 2 MPa and a temperature of 300 °C. It can be seen clearly that the nozzle exit diameter has a significant influence on the particle velocity. There exists an optimal value of nozzle exit diameter for the maximum acceleration of particles. It is about 5 mm under the given conditions. On the other hand, this optimal value is the same for particles with different diameters.

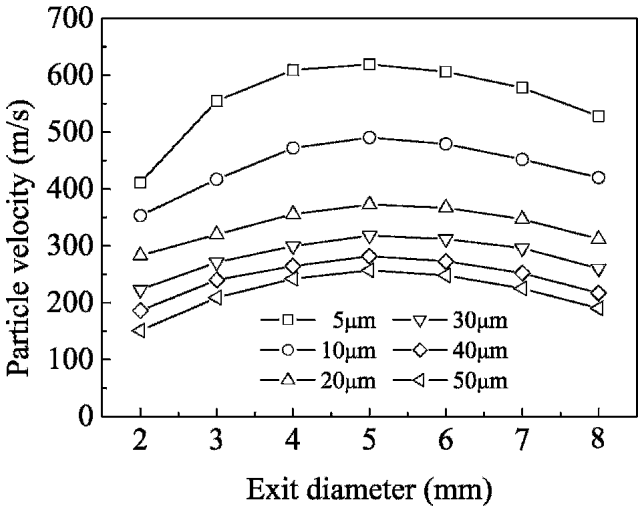

Fig. 4 Effect of nozzle exit diameter on the velocity of particles with different sizes using N_2 at a pressure of 2 MPa and a temperature of 300 °C

According to aerodynamic principles (Ref 4), the expansion ratio of a nozzle, defined as the ratio of the area of the nozzle exit to the throat, will influence the acceleration of gas and then the particles. Although the optimal expansion ratios of a nozzle with a divergent section length of 100 mm obtained through one-dimensional model analysis for the particle acceleration at nozzle exit using N_2 and He (Ref 4), are about 4.7 and 1.7, respectively, the previous study showed that the ratio is about 4 for the nozzle with a divergent section length of 100 mm using either N_2 or He (Ref 10), whereas in this study the ratio is about 6.25 for the nozzle with a divergent section length of 40 mm using N_2. A further study showed that the ratio is still about 6.25 using He. It should be pointed out that in this and previous studies (Ref 10) the optimal exit diameter is between 4 and 5 mm. However, a small change in exit diameter from 4 to 5 mm will cause a big difference in the expansion ratio from 4 to 6.25. Therefore, it is considered that the shock waves that form outside the nozzle exit will exert a significant effect on particle acceleration, especially when a short nozzle is used. Figure 5 shows a typical result for the gas velocity distribution outside the nozzle with an exit diameter of 5 mm using N_2 at a pressure of 2 MPa and a temperature of 300 °C. It is clear that shock waves are formed before the substrate. When a particle passes through these shock waves, the acceleration rate of the particle will be decreased owing to the significant decrease in gas velocity, which will be more remarkable for the particle with a diameter of less than ~5 μm.

Theoretically, one expansion ratio for a specific nozzle and gas corresponds to a designated exit Mach number. The larger the Mach number, the higher the gas velocity will be at the nozzle exit. However, the shock waves will decrease the gas velocity noticeably outside the nozzle as the expansion ratio is

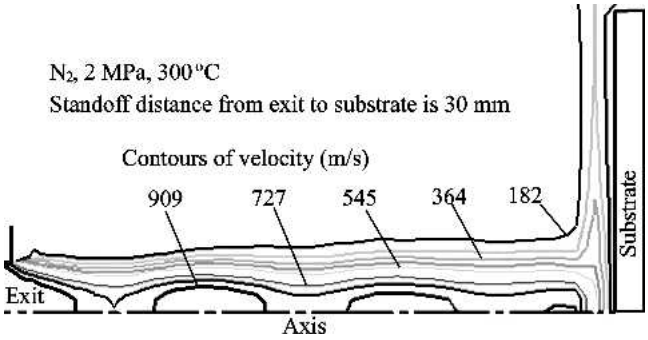

Fig. 5 Contours of gas velocity outside the nozzle exit with an exit diameter of 5 mm using N_2 at a pressure of 2 MPa and a temperature of 300 °C

large enough. Jodoin (Ref 9) also reported that a limitation exists for an exit Mach number from 1.5 to 3 for cold spraying using air. In this study, the optimal exit Mach number for maximum particle velocity at a standoff distance of 30 mm is about 3.4 for N_2 and 5.4 for He.

3.2 Effect of Gas Conditions on Particle Acceleration

Figure 6 shows the effect of N_2 temperature on the particle velocity with different particle sizes under a pressure of 2 MPa. It is seen that the particle velocity increases with increasing gas inlet temperature. Figure 7 shows the effect of N_2 pressure on the particle velocity at the standoff distance with different particle sizes under a temperature of 300 °C. It is seen that the particle velocity also increases with increasing gas inlet pressure. On the other hand, from Fig. 8 it can also be seen that the particles are accelerated to a higher velocity using He as the accelerating gas compared with N_2 at the same pressure and temperature. These results are consistent with the reported results in Ref 3 to 8. The reason can be simply explained using the equation:

$$V_g = M\sqrt{\gamma R T_g} \quad \text{(Eq 8)}$$

For a given spray nozzle, He yields a higher M than N_2. The specific heat ratios of N_2 and He are 1.4 and 1.66, respectively. The specific gas constants of N_2 and He are 2078.2 and 296.8, respectively. According to Eq 8, the gas velocity of He will be much higher than that of N_2 under the same conditions. Therefore, the particles will be accelerated to a higher velocity when using He than when using N_2. On the other hand, with the increase in gas temperature the gas velocity will be increased and subsequently the particle velocity. As the gas pressure increases, the drag force to the particle will be increased owing to the increase in gas density.

Therefore, a selection of the gas parameters can be conducted following those results. Owing to the limited space, He can be used as the accelerating gas at a relatively high operating pressure and temperature if the cost permits.

3.3 Effects of Powder Size on Particle Acceleration

The previous study showed that particle density, size, and morphology influence its velocity significantly (Ref 10). With

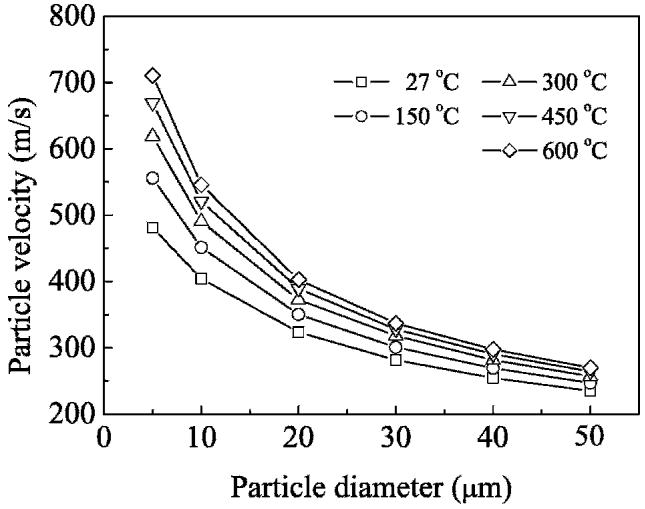

Fig. 6 Effect of N_2 temperature on the velocity of particles with different sizes at a pressure of 2 MPa

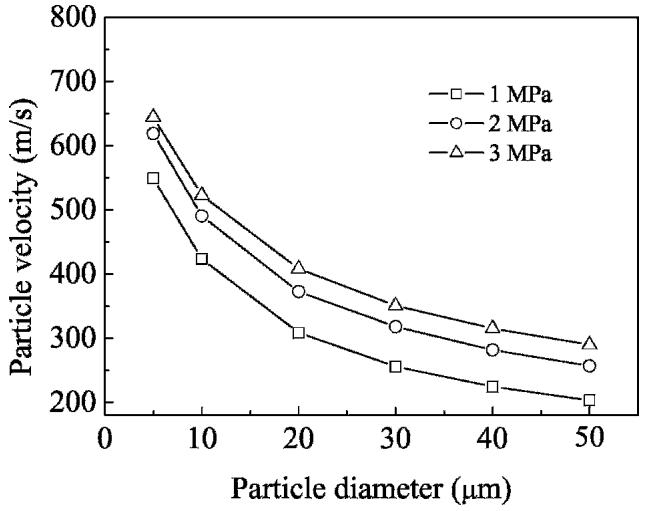

Fig. 7 Effect of N_2 pressure on the velocity of particles with different sizes at a temperature of 300 °C

increasing particle density, particle velocity decreases. With a more irregular shape, the particle can be accelerated more easily. On the other hand, the powder particle size has also been confirmed to be an important factor influencing particle acceleration (Ref 2-10). As shown in Fig. 4 and Fig. 6 to 8, the particle size influences the particle velocity significantly. With the decrease in particle diameter, the particle velocity increases rapidly, especially as the particle diameter is less than ~20 μm.

Therefore, in this study, owing to the limited space, a powder with a relatively small particle size could be used for a successful deposition.

4. Experimental Correlation

4.1 Experimental Procedures

Based on the results presented above, a short cold spray gun was designed and manufactured for use in a limited space, espe-

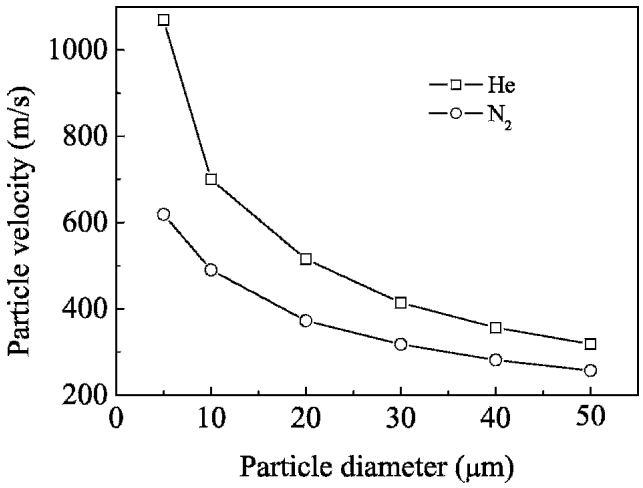

Fig. 8 Effect of gas type on the velocity of particles with different sizes at a pressure of 2 MPa and a temperature of 300 °C

cially for the inner wall of a cylinder or pipe with a total length of no longer than 70 mm in the nozzle axial direction. The schematic diagram of the designed spray gun is shown in Fig. 9. The designed short nozzle has values for the D_i, D_t, D_e, L_u, and L_d of 8, 2, 5, 10, and 40 mm, respectively.

The commercially available copper powder (5 to 48 μm with a medial diameter of 24 μm) was used as feedstock to deposit on the inner wall of a stainless steel pipe (inner diameter 100 mm). Prior to deposition, the substrate was sandblasted to a rough surface.

N_2 was used as an accelerating gas at a pressure of 2 MPa and a temperature of about 300 °C. The standoff distance from nozzle exit to substrate surface was 30 mm.

After deposition, a sample was cut using electrical discharge machining from the pipe and was mounted for polishing. The microstructure was characterized by optical microscopy (MeF3A, Reichert-Jung, Wetzlar, Germany).

4.2 Experimental Results

Figure 10 shows the typical microstructure of a cold-sprayed Cu coating using the designed spray gun. It is seen from Fig. 10(a) that a dense Cu coating could be deposited using the short spray gun in comparison with the conventional cold spray gun (Ref 2, 6, 8). The thickness of the sprayed Cu coating was about 1 mm. The spray particles have experienced intensive deformation to form the splats during deposition, which can be seen clearly in the etched state in Fig. 10(b). It should be pointed out that the deposition efficiency was relatively low owing to the rebound off of large particles. Further study showed a much higher deposition efficiency using He as the driving gas and with copper powder with a particle size of <27 μm. Although the critical velocity for copper was reported to be ~570 m/s by Stoltenhoff et al. (Ref 6), Van Steenkiste et al. (Ref 8) reported a much lower critical velocity for a copper powder with relatively large particles. Therefore, the critical velocity for a specific spray material may be influenced by other underlying factors besides the mechanical properties of the spray material. Consequently, it is reasonable that a dense copper coating can be deposited under

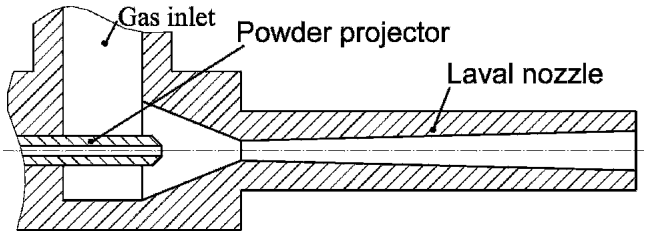

Fig. 9 Schematic diagram of a spray gun designed with a short nozzle according to the simulation results

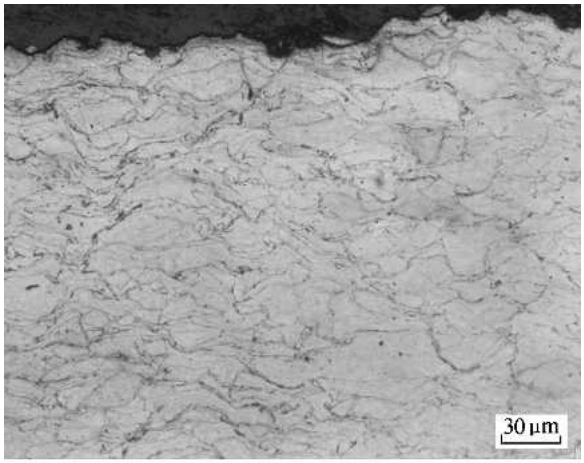

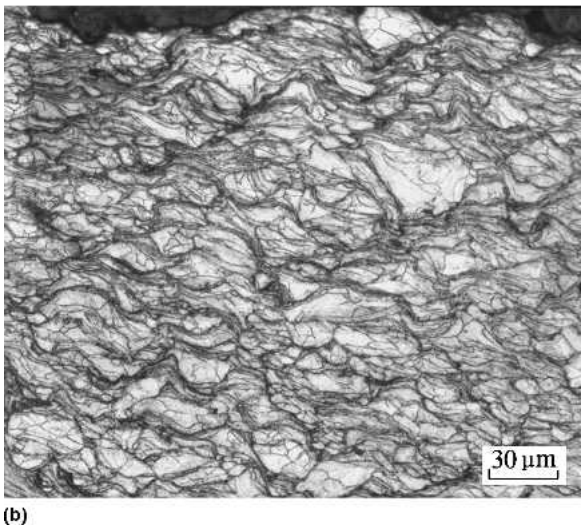

Fig. 10 (a) Typical microstructure of a cold-sprayed Cu coating achieved with the designed short spray gun using N_2 at a pressure of 2 MPa and a temperature of ~300 °C. (b) Etched to reveal the interparticle boundaries

the spray condition of this study because a fraction of the particles reached a velocity higher than the critical one.

According to the above experimental results, it can be considered that the optimal design of the spray gun nozzle for other industrial applications can also be conducted through finite-element analysis. The designed spray gun can meet the need of

the application. Further study is still needed to compare the properties of the deposited Cu coatings with the conventional cold-sprayed coatings and to deposit other materials.

5. Conclusions

Based on the simulation results, it was found that the nozzle expansion ratio, powder size, accelerating gas type, operating pressure, and temperature are the main factors influencing the accelerating behavior of spray particles for a short spray gun nozzle. There exists an optimal expansion ratio of 6.25 for particle acceleration at the standoff distance of 30 mm using either N_2 or He, with a nozzle divergent section length of 40 mm. The spray particles can achieve a higher velocity at a higher pressure and temperature when using He as the accelerating gas. The smaller particles in the particle size range used in this study can be accelerated to a higher velocity. The experiment using the designed short nozzle with a whole gun length of <70 mm confirmed the feasibility of creating an optimal design for a spray gun nozzle that would be used in a limited space. A dense coating could be deposited by the designed short spray gun.

References

1. A. Papyrin, Cold Spray Technology, *Adv. Mater. Process.,* Vol 159, 2001, p 49-51
2. C.-J. Li and W.-Y. Li, Deposition Characteristics of Titanium Coating in Cold Spraying, *Surf. Coat. Technol.,* Vol 167, 2003, p 278-283
3. D.L. Gilmore, R.C. Dykhuizen, R.A. Neiser, T.J. Roemer, and M.F. Smith, Particle Velocity and Deposition Efficiency in the Cold Spray Process, *J. Thermal Spray Technol.,* Vol 8, 1999, p 576-582
4. R.C. Dykhuizen and M.F. Smith, Gas Dynamic Principles of Cold Spray, *J. Thermal Spray Technol.,* Vol 7, 1998, p 205-212
5. K. Sakaki and Y. Shimizu, Effect of the Increase in the Entrance Convergent Section Length of the Gun Nozzle on the High-Velocity Oxygen Fuel and Cold Spray Process, *J. Thermal Spray Technol.,* Vol 10, 2001, p 487-496
6. T. Stoltenhoff, H. Kreye, and H.J. Richter, An Analysis of the Cold Spray Process and Its Coatings, *J. Thermal Spray Technol.,* Vol 11, 2002, p 542-550
7. A.P. Alkhimov, V.F. Kosarev, and S.V. Klinkov, The Features of Cold Spray Nozzle Design, *J. Thermal Spray Technol.,* Vol 10, 2001, p 375-381
8. T.H. Van Steenkiste, J.R. Smith, R.E. Teets, J.J. Moleski, D.W. Gorkiewicz, R.P. Tison, D.R. Marantz, K.A. Kowalsky, W.L. Riggs, P.H. Zajchowski, B. Pilsner, R.C. McCune, and K.J. Barnett, Kinetic Spray Coatings, *Surf. Coat. Technol.,* Vol 111, 1999, p 62-71
9. B. Jodoin, Cold Spray Nozzle Mach Number Limitation, *J. Thermal Spray Technol.*, Vol 11*,* 2002, p 496-507
10. W.-Y. Li and C.-J. Li, Optimization of Spray Conditions in Cold Spraying Based on the Numerical Analysis of Particle Velocity, *Trans. Nonferrous Met. Soc. China,* Vol 11 (Special 2), 2004, p 43-48
11. E. Hämäläinen, N. Kriikka, and G. Barbezat, On-line Optical Diagnostics of a Rotating Internal Diameter Plasma Spray Gun Used for Coating of Cylinder Bores in Automotive Industry, *Thermal Spray 2003: Advancing the Science and Applying the Technology,* C. Moreau and B. Marple, Ed., May 5-8, 2003 (Orlando, FL), ASM International, 2003, p 1249-1253
12. L. Byrnes and M. Kramer, Method and Apparatus for the Application of Thermal Spray Coatings onto Aluminium Engine Cylinder Bores, *Thermal Spray Industrial Applications,* C.C. Berndt and S.Sampath, Ed., June 20-24, 1994 (Boston, MA), ASM International, 1994, p 39-42
13. FLUENT Inc., *FLUENT Manual*, Lebanon, NH, 1999